Minimizing Noise in Distributed Reflector Laser Types Under Optical Injection Locking

Arbnor Berisha, Hendrik Boerma, Ronald Kaiser, Patrick Runge, and Martin Schell, *Member, IEEE*

***Abstract*— Complex coupled distributed feedback (DFB) lasers and sampled grating distributed Bragg reflector (SGDBR) lasers under optical injection locking are investigated to determine lowest noise operation. A noise reduction (frequency and intensity combined) of up to 15 dB was measured utilizing detuned optical injection locking at the relaxation oscillation frequency. Furthermore, 4 dB improvement in frequency noise at 10 kHz offset for higher coupling coefficient DFBs under injection locking was measured. The DFB lasers show more sensitivity to injection locking and have a lower need of injection power while exhibiting better signal to noise ratio compared to an SGDBR.**

***Index Terms*— Diffraction gratings, injection locking, noise measurement, noise reduction, frequency noise, semiconductor lasers, laser noise.**

I. Introduction

THZ communications is getting more and more attention due to the upcoming 6G wireless communication. 6G will cover frequencies in the Terahertz region starting at 100 GHz and reaches up to 3 THz [1]. For optical THz signal generation, signals from two laser sources are combined to a beat signal in a photodiode as demonstrated in [2].

In wireless communication it is known that RF noise and phase noise are the main factors, degrading the error vector magnitude (EVM) and thus limit the maximum achievable data rate in communication links. Utilizing optical injection locking (OIL), the phase noise of the two laser sources can be improved, allowing for an increase link capacity and range [3]. Channel bandwidth in IEEE 802.11 standard of 20-160 MHz and up to 8 GHz for transmission rates of over 20 Gb/s [4] make noise in this offset frequency band and higher important to mitigate now and for future channel bandwidths.

Optical injection locking is a method for synchronizing optical frequencies and phases, which relies on photon-photon interaction, occurring when external light of a first primary laser enters a laser cavity of a secondary laser [5]. The effects of bandwidth enhancement [6] and cavity shift [7] have been discussed.

The major objective of this study is to investigate the suitability of different distributed reflector (DR) laser types and OIL methods for OIL-based signal improvement with complex coupled distributed feedback (DFB) and sampled grating distributed Bragg reflector (SGDBR) secondary lasers.

II. Theoretical Analysis

A. Locking Range

One important characteristic for injection locking is the locking range of the secondary laser. To determine the locking range, we can use the equation [8]:

$$-\kappa\sqrt{1+\alpha_H^2}\sqrt{R_{\mathrm{inj}}} = \Delta\omega_{\mathrm{min}} \leq \Delta\omega \leq \Delta\omega_{\mathrm{max}} = \kappa\sqrt{R_{\mathrm{inj}}} \tag{1}$$

The injection ratio is defined as $\mathbf{R_{inj}} = \mathbf{P_{in}}/\mathbf{P_0}$. The locking range is dependent on the power of the injected light $\mathbf{P_{in}}$, the power of the secondary laser $\mathbf{P_0}$, the coupling coefficient $\boldsymbol{\kappa}$ and the linewidth enhancement factor (LEF) or Henry factor $\boldsymbol{\alpha_H}$.

In Fig. (1) the simulated multielement mirror reflection spectra of SGDBR and DFB laser are shown. It is evident that the reflection bandwidth for a single tone is wider in a DFB, the SGDBR has a much narrower reflection bandwidth in that regard.

III. Cavity Shift

Negative frequency detuned optical injection locking will be referred to as "red locking", positive detuned locking as "blue locking" and little to no detuning as "center locking" for simplicity.

In [9] it is theoretically and experimentally shown that a phase offset $\boldsymbol{\Delta\Phi}$ will manipulate the relaxation resonance peak intensity of semiconductor lasers. It will most closely resemble the primary laser signal shape, and therefore its resonance frequency peak intensity, if there is no phase offset to the secondary laser cavity present. Therefore, frequency noise will be reduced when detuning injected light to a phase offset of zero, given a lower noise primary laser.

A resonance cavity shift $\boldsymbol{\Delta\omega\,(N) = -c\alpha_H g(N - N_{th})/2}$ was observed when injection locking [7], where $\boldsymbol{c}$ is the speed of light, $\boldsymbol{\alpha_H}$ is the henry factor, $\boldsymbol{g}$ is the secondary laser's linear gain coefficient, $\boldsymbol{N}$ is the carrier number and $\boldsymbol{N_{th}}$ is the threshold carrier number. Due to this cavity shift, the phase

Manuscript received 9 April 2024; revised 13 May 2024; accepted 5 June 2024. Date of publication 11 June 2024; date of current version 24 June 2024. This work was supported by the Deutsche Forschungsgemeinschaft (DFG) funded project Mode Locked Laser Based Terahertz Synthesis (MINTS) in the Schwerpunktprogramm 2314 (SPP2314) under Project 469044319. *(Corresponding author: Arbnor Berisha.)*

Arbnor Berisha and Martin Schell are with the Institute of Solid State Physics, Technical University of Berlin, 10623 Berlin, Germany, and also with the Fraunhofer Institute for Telecommunication, Heinrich Hertz Institute, 10587 Berlin, Germany (e-mail: arbnor.berisha@hhi.fraunhofer.de).

Hendrik Boerma, Ronald Kaiser, and Patrick Runge are with the Fraunhofer Institute for Telecommunication, Heinrich Hertz Institute, 10587 Berlin, Germany.

Color versions of one or more figures in this article are available at https://doi.org/10.1109/JQE.2024.3412088.

Digital Object Identifier 10.1109/JQE.2024.3412088

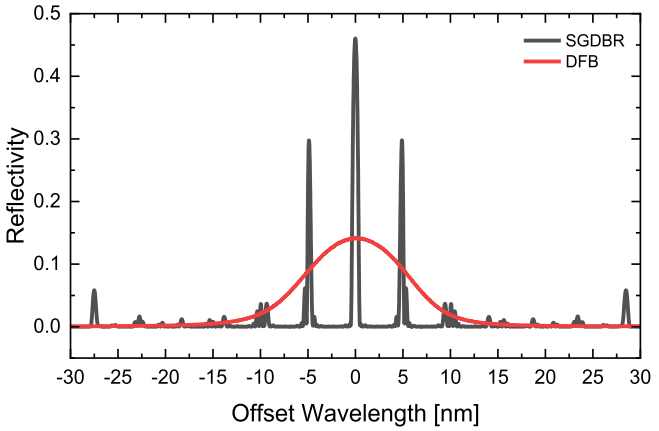

Fig. 1. Simulated multielement mirror reflection spectra of SGDBR and DFB.

Fig. 2. Microscope picture of the complex coupled DFB (left) with 400 μm total device length and SGDBR (right) with 2650 μm total device length.

offset will be zero at the red locking edge. In Equation (2) [6] when setting the detuning $\boldsymbol{\Delta\omega_{inj}} = 0$ (Eq. 5) the phase offset $\boldsymbol{\Delta\Phi}$ does not become zero but has an offset of $\boldsymbol{\Delta\Phi} = \boldsymbol{-tan^{-1}(\alpha_H)}$. This necessitates a negative detuning, as of Equation (5), to compensate the phase offset. Equation (3) [9] shows that given a phase offset of $\boldsymbol{\Delta\Phi = 0}$, the resonance frequency $\boldsymbol{\omega\,(N)}$ aligns with the primary laser frequency $\boldsymbol{\omega_M}$.

$$\boldsymbol{\Delta\Phi = \sin^{-1}\left(-\frac{\Delta\omega_{inj}}{\kappa\sqrt{1+\alpha_H}}\sqrt{R_{inj}}\right) - \tan^{-1}\alpha_H} \quad (2)$$

$$\boldsymbol{\omega\,(N) = \omega_M - \kappa\sin\,(\Delta\Phi)} \quad (3)$$

$$\boldsymbol{G\,(N) = \alpha_L - 2\kappa\cos\,(\Delta\Phi)} \quad (4)$$

$$\boldsymbol{\Delta\omega_{inj} = \omega_M - \omega_S} \quad (5)$$

Here $\boldsymbol{\alpha_L}$ is the cavity loss including mirror losses, $\boldsymbol{\Phi_M}$ is the primary laser phase, $\boldsymbol{\Phi_S}$ *and* $\boldsymbol{\omega_S}$ is the free running secondary laser phase and frequency, $\boldsymbol{\Phi_{cav}}$ is the secondary laser cavity phase, $\boldsymbol{\kappa}$ is the injection coupling. The stationary value of gain $\boldsymbol{G\,(N)}$ is also dependent on $\boldsymbol{\Delta\Phi}$, in contrast to $\boldsymbol{\omega\,(N)}$ the gain reaches its maximum at $\boldsymbol{\Delta\Phi = \pm\pi/2}$ (Eq. 3), also shown in the simulations. This means a decrease in signal strength when red locking, however there is still a significant improvement in SNR. Blue locking on the other hand, where the phase offset is $\pi/2$ at the positive locking edge, was reported in [6] to enhance modulation bandwidth in directly modulated lasers (DML).

IV. Experimental Setup, Results and Discussion

The devices under test (DUTs) are a complex coupled distributed feedback (DFB) laser and a sampled grating distributed Bragg reflector (SGDBR) laser. The fabricated chips are displayed in Fig. (2a).

The DFB exhibits a linewidth of 3.1 MHz and the SGDBR 2.9 MHz. The Linewidth derived from frequency noise is 75 kHz for the DFB and 83 kHz for the SGDBR. The SGDBR has a total length of 2.65 mm, including 800 μm rear grating, 600 μm front grating, 400 μm gain section and 150 μm phase section. The DFB consist of a single 200 μm active region including grating and heater (for wavelength shift) with a total length of 400 μm. Both DUTs where fabricated with a butt-joint regrowth epitaxial structure [10] on the same Fraunhofer HHI dedicated wafer.

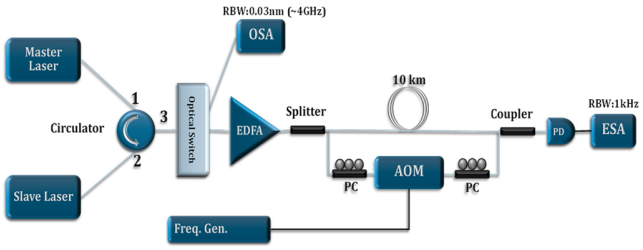

Fig. 3. Schematic of measurement setup for linewidth and optical spectrum, where OSA and ONA are on the same slot.

The DFBs have a smaller tuning range of about 4 nm [11]. SGDBRs have been shown to be tunable up to 53 nm [12].

An optical and electrical spectrum is necessary to explore the properties of the devices being tested. The measuring setup consists of a reflection type injection locking setup with a 200 kHz linewidth tunable primary laser as shown in Fig. (2b). Light from the injection locked secondary laser is sent to the Anritsu MS9740B optical spectrum analyzer (OSA) for optical, the Sycatus A0040A optical noise analyzer (ONA) for frequency noise evaluation and the R&S FSW67 for self-heterodyne linewidth measurement.

Under injection locking, a SGDBR and a complex coupled DFB laser are being analyzed. Both lasers contain the same active section stack and are manufactured on the same Fraunhofer HHI dedicated wafer. Detuning the injected light was achieved with the tunable primary laser.

Frequency noise close (up to 20 MHz) to the signal frequency are assessed using ONA measurements. Linewidth measurements are done with an electrical spectrum analyzer (ESA). The injection locked secondary laser signal passes through the circulator to a self-heterodyne interferometry to the ESA. The signal is split in two paths, the first path containing a delay line of 10 km fiber and the second path an acoustic optic modulator (AOM). The AOM shifts the signal for 80 MHz. Finally, both signals are combined in a photodiode, its electrical signal is then evaluated with an ESA and the linewidth is determined (Fig.4). The power of the lasers are too low to see changes in higher offset frequencies than shown in Fig.4 using the self-heterodyne setup.

For an investigation of the behavior of the DUTs under injection locking, injected light is detuned from the negative edge to the positive edge of the locking range of each laser. Injection power from the primary laser is swept in a 14 dB range into the DUTs.

The optical spectra in Fig. 3 shows the effects of detuned optical injection on noise. Detuning from -15 GHz to $+5$ GHz was measured and plotted. A red locked DFB showed a noise reduction of 10 dB (from -32 dBc/nm to -42 dBc/nm at a resolution of 0.03nm) to a free running and 15 dB (-31 dBc/nm to -46 dBc/nm) to a blue locked regime for a detuning from $+5$ GHz to -15 GHz at a -12 dB injection

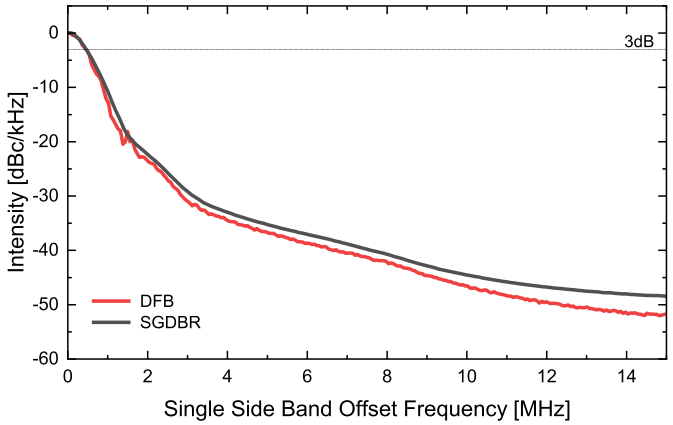

Fig. 4. Measured spectrum of an injection locked DFB and SGDBR normalized to carrier power with a resolution bandwidth of 1 kHz.

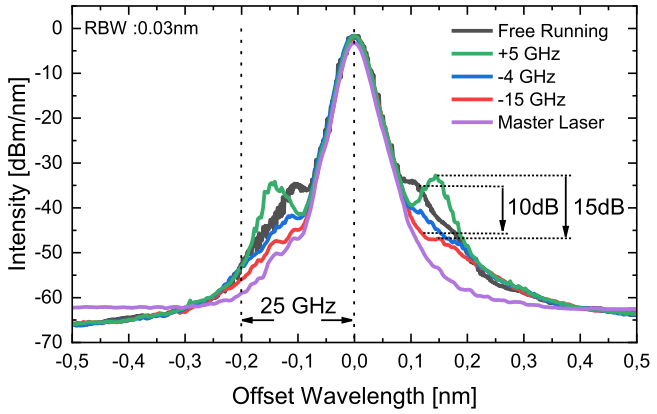

Fig. 6. Measured spectrum of a DFB with detuned injection light from −15 GHz to 5 GHz at an injection ratio of −12 dB.

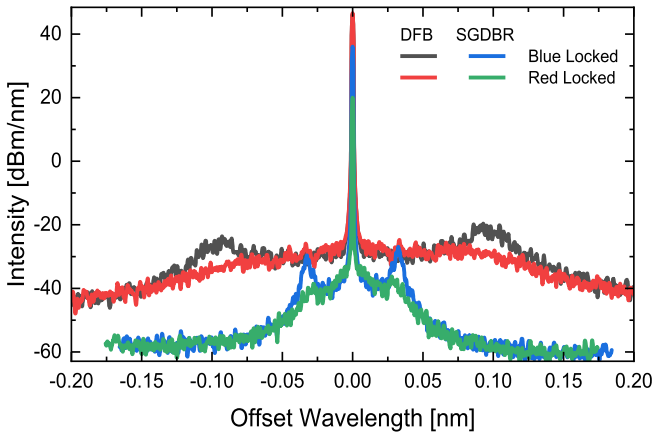

Fig. 5. Simulated spectrum of DFB and SGDBR with detuned injection light.

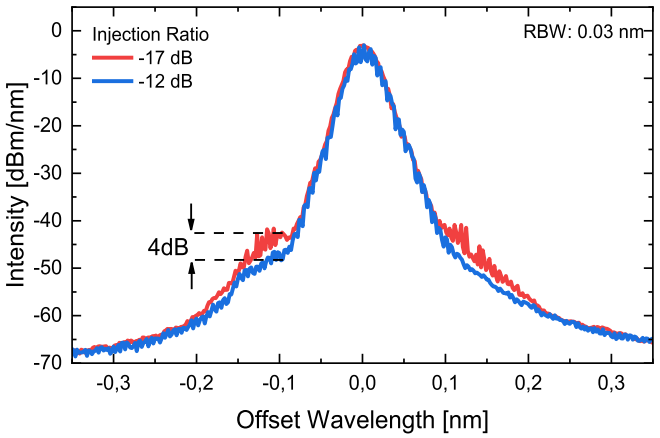

Fig. 7. Measured spectrum of an injection ratio increase for a DFB with −15GHz detuned injection signal.

ratio at the relaxation resonance frequency. In [13] a noise reduction for injection locking of about 15 dB for VCSELs was shown and in [14] about 14 dB for quantum well laser diodes for injection ratios of 10 and −9 dB, respectively.

Both lasers exhibit increased relaxation resonance peaks when injection locked with positive frequency detuning and a reduction when negatively detuning the injected light to the secondary laser free running frequency according to simulations (Fig. 5). Depending on how the injected light is detuned to the secondary laser frequency within the locking range, frequency noise close to the signal wavelength, will vary as shown in measurements (Fig. 6). In [15] a theoretical investigation of frequency noise in quantum cascade lasers was conducted and reported the observed effect of Fig. 5. The damping of relaxation oscillation peaks can be seen in measurements for the DFB but only in simulations for SGDBRs (Fig. 6), due to insufficient resolution in spectral measurements for frequencies over 20 MHz.

While injection locking effects are correctly represented in simulations, linewidths could not reflect measurement data. Linewidths are 3 orders of magnitude smaller in simulations than in measurements, including the primary laser. The Simulations in Fig. 5 hence show very narrow lines compared to the measurements.

Relaxation resonance peaks will rise in intensity continuously from the negative to the positive locking edge. A demonstration of this behavior can be seen in Fig. 5. Increasing the injection ratio causes noise to decrease independent of detuned injection (Fig. 7), this indicates that the Bogatov effect plays a role in detuned optical injection locking.

The Bogatov effect is a parametric amplification and damping depending on detuning between pump and probe signal [16], [17]. The satellite peaks in Fig. 5 show that a negative frequency detuning results in amplification while a positive frequency detuning results in intensity dampening, as there is an asymmetry in intensity between satellite peaks

In a red locked regime, the primary laser is negatively frequency detuned to the secondary laser signal, resulting in an amplification of the primary laser signal inside the cavity. The injection ratio is effectively increased in this regime. In a blue locked regime, the primary laser power is decreased, thereby decreasing the effective injection ratio. The Bogatov effect further increases effects previously described by the cavity shift, by changing the effective R_{inj}.

The injected power reaching the active region differs depending on the laser type, making the sensitivity to OIL different (Fig.9). When using the same primary laser power, the DFB active region receives more power than the SGDBRs do.

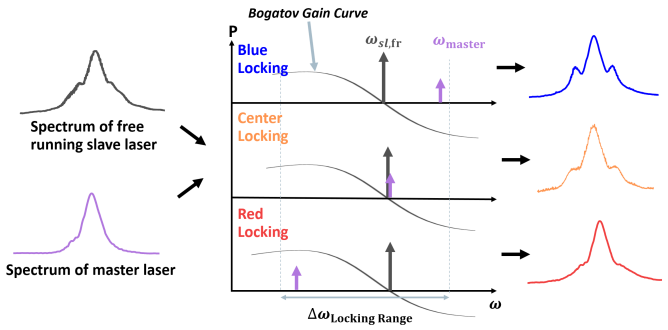

Fig. 8. Illustration of Bogatov effect and cavity shift during injection locking.

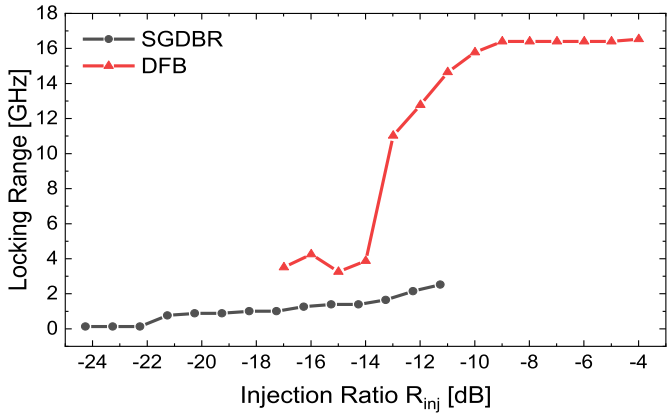

Fig. 9. Measured locking range of a DFB and SGDBR as a function of effective injection ratio. Equal primary laser power was injected.

The reflectivity of the SGDBR gratings is higher and thus will reflect more of the injected light (Fig. 1). Contrary to DFBs, the optical losses are higher, because the injected light needs to pass lossy passive sections until it reaches the amplifying gain region (Fig. 9). The effective R_{inj} is hence increased for the DFBs and, thus, the locking range (Eq. 1). As a result of the narrower reflection bandwidth for a single tone the locking range of SGDBRs is smaller. A narrower reflection bandwidth causes the detuned injected light to resonate less strongly, which lowers the intensity of the light inside the cavity and reduces the injection ratio and locking range (Eq. 1) (Fig. 9). The DFB hence requires lower power consumption for the primary laser during an injection locking operation.

The estimated LEF is 2.05 for both DFB and SGDBR. All OIL measurements are conducted in the stable locking range of the lasers. The locking range for both laser types has been measured, using an electrical spectrum analyzer with a resolution bandwidth of 1 kHz, in Fig. 9 for a span of effective injection ratios.

DBR type lasers typically exhibit a smaller linewidth than DFBs, due to their higher length and reflection outside the active region. Longer lasers result in a longer round-trip time and reflections outside the active zone indicate a higher finesse reflection cavity. However, with injection locking, the linewidth will lock to the primary laser linewidth regardless of secondary laser linewidth [18]. The electrical spectrum is measured using a self-heterodyne setup, which is used to determine the linewidth of the DUTs. It is possible to measure

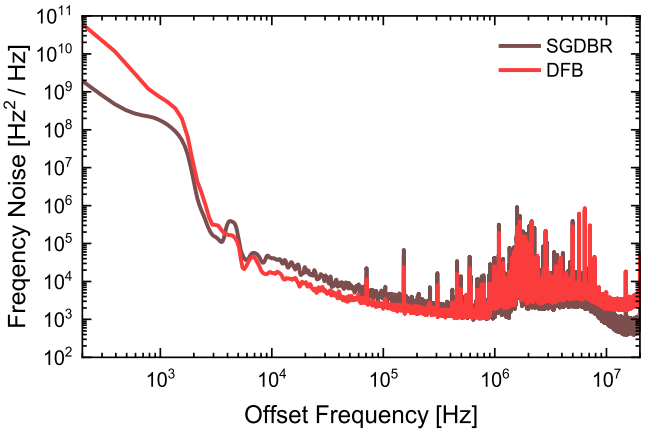

Fig. 10. Measured frequency noise of SGDBR and DFB with $\kappa \sim 500$ cm^{-1} injection locked.

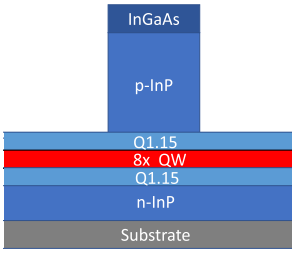

Fig. 11. Schematic of epitaxial growth for SOA in the SGDBR and DFB.

TABLE I
CALCULATED κ FOR DIFFERENT GRATING ETCH DEPTHS

Etch depth [nm]	DFB κ [cm^{-1}]	SGDBR κ [cm^{-1}]
20	66 + i58	515
40	555 - i400	601
170	539 - i100	670

frequency noise close to the peak at frequency offsets of up to 20 MHz (Fig.8). Under optical injection locking, all lasers exhibit the same linewidth, although frequency noise varies at offset frequencies (Fig. 4 & 10). In comparison to the tested SGDBRs, the DFBs have demonstrated a lower frequency noise by about 3 dB at 10 kHz offset (Fig. 10). The calculated coupling coefficient of different etch depths for complex coupled DFBs and SGDBRs are shown in Tab. I. The epitaxial growth of the SOA for the SGDBR and the DFB are shown in Fig. 11.

Simulations suggest that a higher coupling coefficient κ results in a lower frequency noise by increasing locking range and lowering output coupling of laser light (Fig. 12) [19].

Complex coupled DFBs can have a high κ and low reflection therefore can show lower intensity in relaxation resonance peaks. Furthermore, because they are short in length and therefore have a short round-trip time, the peak strength of the relaxation resonance is reduced by raising the relaxation resonance frequency [20]. A higher coupling is achieved through a deeper etch, which will result in higher internal reflection and lower output and higher internal power. The grating etch depth is equally deep for both tested laser

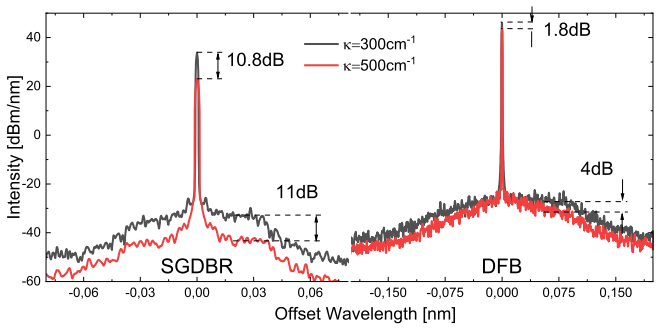

Fig. 12. Simulated spectrum of two SGDBRs (left) & DFBs (right) with different κ. Point of reference taken at resonance relaxation oscillation frequency.

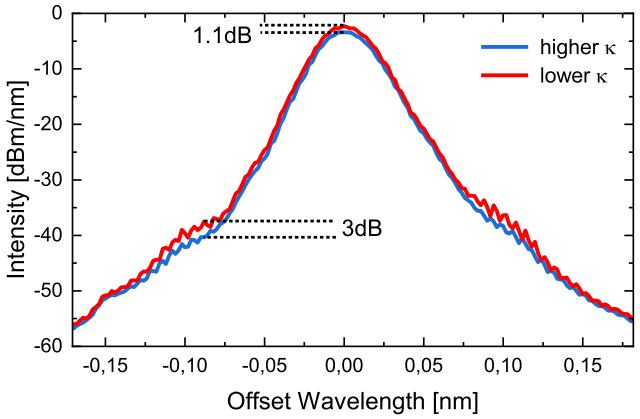

Fig. 13. Measured injection. locked DFB lasers at −15GHz detuning with different κ (estimated to be $\sim$ 300 & 500 cm^{-1}) under the same injection ratio of −9 dB.

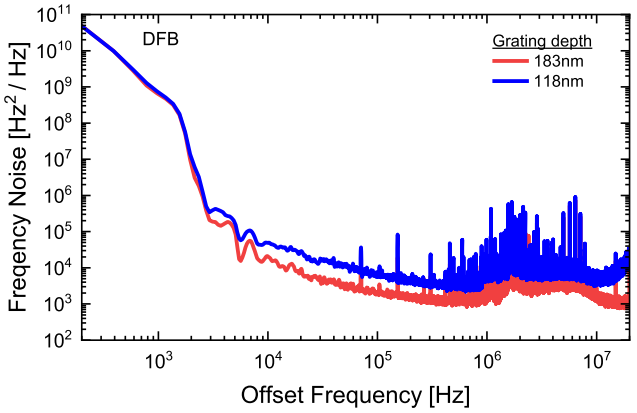

Fig. 14. Measured frequency noise of DFB injection locked at −14 dB eff. injection ratio for different grating depths.

types. Compared to lower κ DFBs, higher κ DFBs shows a 3 dB reduction in the optical spectrum (Fig.13) validating the simulation results (Fig. 12). Moreover, 4 dB in frequency noise at 10 kHz offset (Fig. 14) can be observed, while SGDBRs show no meaningful reduction (Fig. 15). The SGDBR has a low locking range and an already high reflection on front and rear grating, an increase in κ will not increase the locking range or reflectivity significantly, on the opposite site a lower κ will allow for a bit more injection light to enter the cavity which leads to a little increase in effective injection ratio

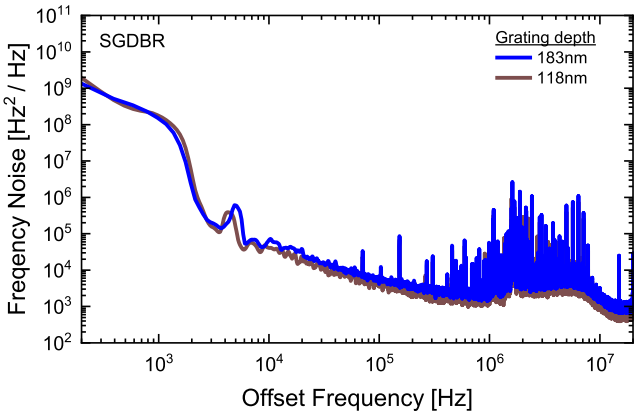

Fig. 15. Measured frequency noise of SGDBR injection locked at −14 dB eff. injection ratio for different grating depths.

thereby reducing noise. For complex coupled DFBs sensitivity to optical feedback or in this case optical injection is also higher than in high κ index coupled DFBs [21].

V. Conclusion

A complex coupled DFB and an index coupled SGDBR laser have been investigated under optical injection locking. The DFB shows a higher locking range under the same optical injection power compared to the SGDBR. However, the SGDBR shows a lower sensitivity for optical injection, due to its high and narrow reflection spectrum for a single tone. SGDBRs have a larger footprint and have different front and rear gratings. A higher reflection on the rear grating in transmission type injection locking, reduces the injected light power. A higher input power is hence required to achieve the same injection ratio. This makes transmission type injection locking less energy-efficient than reflection type injection locking. The DFB has a smaller footprint and can be injection locked from either side using the same input power, due to the same reflectivity on both sides. Reflection type injection locking requires a multi-mode interferometer (MMI) and a 180° waveguide bend to achieve on chip integration. When considering the losses of the MMI and the bend, transmission type injection would yield more input power into the laser. Furthermore, the MMI creates a second cavity due to back reflections and thereby introduces additional noise.

A high κ improves frequency noise in DFB lasers and increases the locking range. In addition, detuned optical injection showed good results in decreasing noise at higher offsets to the carrier frequency. In comparison with blue locking, red locking improves noise by up to 15 dB for the secondary laser. However, the main mode linewidth is solely determined by the primary laser linewidth.

When injection locking DFBs and SGDBRs it is crucial to decide, if fast modulation (blue locking) or low noise operation (red locking) is the goal, as the detuning is opposite and has a contrary effect to the other purpose (e.g. lower bandwidth modulation or higher noise operation).

A red locked complex coupled DFB with a deeply etched grating showed to be the best choice in regards to noise and sensitivity to OIL for purity signal generation components.

REFERENCES

[1] T. S. Rappaport et al., "Wireless communications and applications above 100 GHz: Opportunities and challenges for 6G and beyond," *IEEE Access*, vol. 7, pp. 78729–78757, 2019.

[2] S. Jia et al., "Integrated dual-laser photonic chip for high-purity carrier generation enabling ultrafast terahertz wireless communications," *Nature Commun.*, vol. 13, no. 1, p. 1388, Mar. 2022.

[3] J. C. Scheytt, D. Wrana, M. Bahmanian, and I. Kallfass, "Ultra-low phase noise frequency synthesis for THz communications using optoelectronic PLLs," in *Proc. 3rd Int. Workshop Mobile THz Syst. (IWMTS)*, Essen, Germany, Jul. 2020, pp. 1–4.

[4] Y. Ghasempour, C. R. C. M. da Silva, C. Cordeiro, and E. W. Knightly, "IEEE 802.11ay: Next-generation 60 GHz communication for 100 Gb/s Wi-Fi," *IEEE Commun. Mag.*, vol. 55, no. 12, pp. 186–192, Dec. 2017, doi: 10.1109/MCOM.2017.1700393.

[5] H. L. Stover and W. H. Steier, "Locking of laser oscillators by light injection," *Appl. Phys. Lett.*, vol. 8, no. 4, pp. 91–93, Feb. 1966.

[6] E. K. Lau, L. Jie Wong, and M. C. Wu, "Enhanced modulation characteristics of optical injection-locked lasers: A tutorial," *IEEE J. Sel. Topics Quantum Electron.*, vol. 15, no. 3, pp. 618–633, Jun. 2009.

[7] A. Murakami, K. Kawashima, and K. Atsuki, "Cavity resonance shift and bandwidth enhancement in semiconductor lasers with strong light injection," *IEEE J. Quantum Electron.*, vol. 39, no. 10, pp. 1196–1204, Oct. 2003.

[8] L. A. Coldren, S. W. Corzine, M. L. Masanovic, and K. Chang, *Diode Lasers and Photonic Integrated Circuits*. Hoboken, NJ, USA: Wiley, 2012, p. 321.

[9] P. Spano, S. Piazzolla, and M. Tamburrini, "Frequency and intensity noise in injection-locked semiconductor lasers: Theory and experiments," *IEEE J. Quantum Electron.*, vol. QE-22, no. 3, pp. 427–435, Mar. 1986.

[10] J. W. Raring et al., "Advanced integration schemes for high-functionality/high-performance photonic integrated circuits," *Proc. SPIE*, vol. 6126, Feb. 2006, Art. no. 61260H.

[11] K. Xu et al., "Improved range tunability of DFB lasers based on REC technique under injection current," *IEEE J. Quantum Electron.*, vol. 57, no. 2, pp. 1–7, Apr. 2021.

[12] M.-H. Lee, F. Soares, M. Baier, M. Möhrle, W. Rehbein, and M. Schell, "53 nm sampled grating tunable lasers from an InP generic foundry platform," *Proc. SPIE*, vol. 11356, Apr. 2020, Art. no. 1135605.

[13] L. Chrostowski, X. Zhao, and C. J. Chang-Hasnain, "Microwave performance of optically injection-locked VCSELs," *IEEE Trans. Microw. Theory Techn.*, vol. 54, no. 2, pp. 788–796, Feb. 2006.

[14] T. B. Simpson, J. M. Liu, and A. Gavrielides, "Bandwidth enhancement and broadband noise reduction in injection-locked semiconductor lasers," *IEEE Photon. Technol. Lett.*, vol. 7, no. 7, pp. 709–711, Jul. 1995.

[15] X.-G. Wang, B.-B. Zhao, F. Grillot, and C. Wang, "Frequency noise suppression of optical injection-locked quantum cascade lasers," *Opt. Exp.*, vol. 26, no. 12, pp. 15167–15176, Jun. 2018.

[16] A. Bogatov, P. Eliseev, and B. Sverdlov, "Anomalous interaction of spectral modes in a semiconductor laser," *IEEE J. Quantum Electron.*, vol. QE-11, no. 7, pp. 510–515, Jul. 1975.

[17] P. Runge, R. Elschner, C.-A. Bunge, and K. Petermann, "Extinction ratio improvement due to a Bogatov-like effect in ultralong semiconductor optical amplifiers," *IEEE J. Quantum Electron.*, vol. 45, no. 6, pp. 629–636, Jun. 2009.

[18] A. Berisha, H. Boerma, P. Runge, and M. Schell, "Optical injection locking of different distributed reflector laser types," in *Proc. Adv. Photon. Congr.*, Busan, South Korea, 2023, pp. 1–2, Paper ITh2B.3.

[19] E. H. Huntington, T. C. Ralph, and I. Zawischa, "Sources of phase noise in an injection-locked solid-state laser," *J. Opt. Soc. Amer. B, Opt. Phys.*, vol. 17, no. 2, p. 280, Feb. 2000.

[20] K. Vahala and A. Yariv, "Semiclassical theory of noise in semiconductor lasers—Part II," *IEEE J. Quantum Electron.*, vol. QE-19, no. 6, pp. 1102–1109, Jun. 1983.

[21] M. F. Alam, M. A. Karim, and S. Islam, "Effects of structural parameters on the external optical feedback sensitivity in DFB semiconductor lasers," *IEEE J. Quantum Electron.*, vol. 27, no. 6, pp. 424–433, Mar. 1997.

Arbnor Berisha received the bachelor's and master's degrees in physics from the Technical University of Berlin (TU Berlin), Germany, in 2017 and 2022, respectively. He worked on monolayer semiconductor interaction with light with the Institute for Theoretical Physics, Workgroup Nonlinear Optics and Quantum Electronics, TU Berlin. At the Fraunhofer Heinrich Hertz Institute (HHI), he worked on multiple quantum well structures including polarization diverse photodiodes and avalanche photodiodes. He is currently a Research Associate on THz generation through beat signal generation and FMCW LiDAR with TU Berlin in close cooperation with the Fraunhofer HHI. His research interests include MQW structures as well as InP-based laser structures with low linewidth and high power.

Hendrik Boerma received the M.Sc. degree in electrical engineering from the Technical University of Berlin, Germany, in 2019. He is currently pursuing the Ph.D. degree with the Department Photonics InP and RF, Fraunhofer Heinrich Hertz Institute (HHI). Since 2019, he has been a Research Associate with the Department Photonics InP and RF, HHI. His research interests include the design, and fabrication of photonic integrated waveguide structures, photodetectors, and lasers based on InP.

Ronald Kaiser, photograph and biography not available at the time of publication.

Patrick Runge received the Dipl.-Ing. degree in computer science and the Ph.D. degree in electrical engineering from the Technical University of Berlin, Germany, in 2005 and 2010, respectively. From 2005 to 2007, he was with Hymite GmbH, where he was involved in the RF design and measurement of optoelectronic packages for optical communication. In 2007, he returned to the Technical University of Berlin to pursue the Ph.D. degree, where he investigated nonlinear effects and applications of ultralong semiconductor optical amplifiers. After finishing the Ph.D. degree, he worked from 2010 to 2011 for a patent attorney. Since 2011, he has been with the Fraunhofer Heinrich Hertz Institute (HHI), where he is engaged in the development and fabrication of photodetectors and photonic integrated circuits based on InP. He is currently the Head of the InP and RF Department as well as the Head of the Modulators and Detector Group, HHI. He serves regularly for technical program committees of conferences, such as IEEE/Optica OFC, ECIO, Optica APC, and CSW-IPRM. Since 2020, he has been an Associate Editor of IEEE/OPTICA JOURNAL OF LIGHTWAVE TECHNOLOGY.

Martin Schell (Member, IEEE) received the Dipl.-Phys. degree from RWTH Aachen, Aachen, Germany, in 1989, and the Dr.rer.nat. degree from the Technical University of Berlin, Berlin, Germany, in 1993. He spent one year as a Visiting Researcher with Tokyo University, Tokyo, Japan. From 1996 to 2000, he was a Management Consultant with Boston Consulting Group, Boston, MA, USA. From 2000 to 2005, he was a Product Line Manager and then the Head of Production and Procurement with Infineon Fiber Optics, Munich, Germany. He is currently a Professor of optic and optoelectronic integration with the Technical University of Berlin and the Director of the Fraunhofer Heinrich Hertz Institute. From 2015 to 2021, he was a Board Member of the European Photonics Industry Consortium (EPIC). He is a member of the Photonics21 Board of Stakeholders. He is the Chair of the Board of the Competence Network Optical Technologies Berlin/Brandenburg (OptecBB).